

Optical and Structural Properties of Copper Doped Zinc Oxide thin films Prepared Via Spray Pyrolysis Method.

M. TOUATI TLIBA^{a,b}, **B. Benhaoua**^{a,b}

^a Lab. VTRS, Faculty of Science & Technology, Univ. El-Oued, El-Oued 39000, Algeria

^b Unité de Développement des Energies Renouvelables dans les Zones Arides, El oued 39000, Algeria

^c *Centre National de Recherche en Sciences des Matériaux Tunisie*

Abstract

Un doped and copper doped ZnO (0-5 wt.%) were synthesized by spray pyrolysis technique (homemade) annealed at 375°C. Zinc acetate and copper chloride were used as sources precursor of ZnO and Cu doping, respectively. Optical and structural properties of elaborated thin films were examined by using UV-visible and X-ray diffraction. The optical study indicate that the average transmittance of all samples was more than 81% in the visible region and become more transparent after doping. Optical gap energy was observed to vary between 3.25 - 3.28eV. The structural analysis showed formation a hexagonal wurtzite structure ZnO with a strong (002) preferred orientation except (for 0.0 and 1.5 wt%), while the crystallite size is estimated 23 to 29nm for 0-5wt.% Cu doped ZnO thin films.

Key words : Thin films ; Cu doped ZnO ; Spray pyrolysis ; X-ray diffraction .

1. Introduction

Zinc oxide (ZnO) is one of the most important semiconductor materials , which has attracted a lot of scientific attention due to its several applications such as, light emitting diodes [1], gas sensors [2], solar cells [3] transparent conducting contacts [4], energy storage devices [5], electronic devices [6], liquid crystal displays [7], photo detection [8]. It has wide band gap (3.3 eV) with a large exciton binding energy (60 meV) at room temperature [9, 10] and own the property of transparent conducting oxides (TCO) which are widely used in various transparent electronics applications [11]. As thin films ZnO can be deposited by several techniques such as chemical precipitation method [12], sol-gel [13], chemical bath deposition (CBD) [14], Co-precipitation [15] and spray pyrolysis [16]. Among these methods, more focuses, particularly, on the spray pyrolysis technique because of its advantages such as simplicity, safety and low cost of the equipments for thin films deposition. Use of moving nozzle coupled with spray pyrolysis was proced on glass substrate leading to relatively homogeneous composition and fine microstructure with high quality [17]. Also possibilities

of large-scale area deposition, low temperature processing and direct control of film thickness are feasible. Doped ZnO with little amount of several elements was an attracted subject for researchers. It is well known that doping with aluminum was to obtain a conducting transparent ZnO [18]; whereas doping with Cooper, in pervious study [13], was to ameliorate the sensitivity for the gas detection trough the augmentation of the specific reactive surface. As well, Mn doping regarded as an ideal material for short wavelength magneto-optical applications due to its the thermal solubility of Mn into the ZnO and large band gap [19]. While, doped Lanthanum, it enhances in the removal of the ions copper from water solutions [17], etc...

The aim of this work is to focus more on Cu doping effect, in the range of concentration (0-5 Wt. %) in the sprayed solution, on optical, structural and morphological properties of synthesized ZnO via a spray pyrolysis technique with moving nozzle [17]. Outcome of Cu doping concentration stepped as (0.0, 0.5, 1.5, 2.0 and 5.0wt. %) on optical, structural and of ZnO thin films deposited onto glass substrate at temperature up to 375°C will be investigated. All elaborated samples of Cu doped ZnO thin films and undoped were characterized using UV-visible spectroscopy, X-ray diffraction (XRD) and scanning electron microscopy (SEM) techniques, respectively.

2. Experimental methods

2.1. Synthesis of thin films ZnO

In this study, 0-5wt% Cu doped ZnO thin films were prepared via spray pyrolysis technique. For the preparation of thin films, zinc acetate dehydrate ($\text{Zn}(\text{CH}_3\text{COO})_2 \cdot 2\text{H}_2\text{O}$) and copper chloride ($\text{CuCl}_2 \cdot 7\text{H}_2\text{O}$) were used as sources for ZnO and Cu dopant, respectively. First of all, zinc acetate dehydrate (0.5 M) were prepare by dissolving zinc acetate amount of 2.19 g in 20 ml double distiller water and methanol solution in a volume ratio (1/2:1/2). Some drops of acetic acid (CH_3COOH) were added into solutions as stabilizer and the mixture stirred on magnetic for 90min at 50 C° under vigorous stirring till getting a clear and homogeneous colorless solutions. For Cu doped ZnO, the molar percentages doping of Cu/Zn (0.5-5 wt.%) were added to the initial above solutions with kept in magnetic stirrer for the same time and temperature (90 min at 50 C°) until become a clear and homogeneous bleu solutions too. All our thin films samples deposited on heated 375C°glass slides (ref: 217102) during 12 min with a spray rate of the solution about 5mL/min with keeping distance nozzle-substrate equal 5 cm.

2.3. Characterization Techniques

The optical transmittance spectra of all samples were measured using a UV-Visible spectrophotometer (Shimadzu, Model 1800) in the region of 300-900 nm. X-ray diffraction of all thin films recorded using (XRD) with $\text{CuK}\alpha$ radiation ($\lambda=1.5418 \text{ \AA}$).

3-Results and discussion

3.1 Optical analysis

Fig.1 illustrates the optical transmittance spectra of thin films for different concentrations doping (0, 0.5, 1.5, 2 and 5 wt%) measured in range 300-900 nm. All the samples have transmittance of about (81-91%) in the wavelength range higher than 400nm, transmittance values after doping are greater than undoped value, this increase is may be assigned to high-quality of the thin films with feeble absorption losses or scattering [20]. as reveled by the feeble Urbach energy see table 1 and also based on calculated dislocation ($\delta=1/D^2$) which means the number of (lines/m²) on the surface of the samples. It reveals that the doped sample at 2 wt% has the minimum value, then has a minimum scattering. Transmittance values are mentioned in Table 1. While at region wavelength lower 400 nm, an abrupt fall of the transmittance, for all the thin films, can be seen, exhibiting the onset fundamental absorption due to the transition between the valence band and conduction one. The energy band gap was calculated using well know Tauc equation:

$$(\alpha h\nu)^2 = B(h\nu - E_g)$$

where E_g and $h\nu$ are the band gap and the photon energy, respectively; α is the absorption coefficient and B is a constant. The variation of $(\alpha h\nu)^2$ plot as a function of $(h\nu)$ is shown in Fig.2. The optical band gap E_g of all the samples are obtained by extrapolating the linear part of the $(\alpha h\nu)^2$ vs $(h\nu)$ to the energy axis at $(\alpha h\nu)^2=0$. Fig. 2 displays the deduction of E_g values which are found to be about (3.25-3.28 eV) as listed in Table1. A decreasing in the optical band gap for the Cu doped samples compared to the undoped one (3.275eV) in the cases of (0.5, 1.5 and 2 wt. % of Cu) then increase for 5wt. % Cu doping. Such reduce may be caused by sp-d exchange interactions between the band electrons of ZnO as well as the localized d-electrons of Cu⁺² ions substituting Zn⁺² ions [21 , 22-25]. On the other hand, the decrease in the band gap by Cu doping is moreover attributed to the strong p-d mixing of O and Cu [26]. Whereas the increase from 3.268 to 3.284 eV in the case for 5Cu%. This increase in the value of E_g may originated from Burstein-Moss effect .

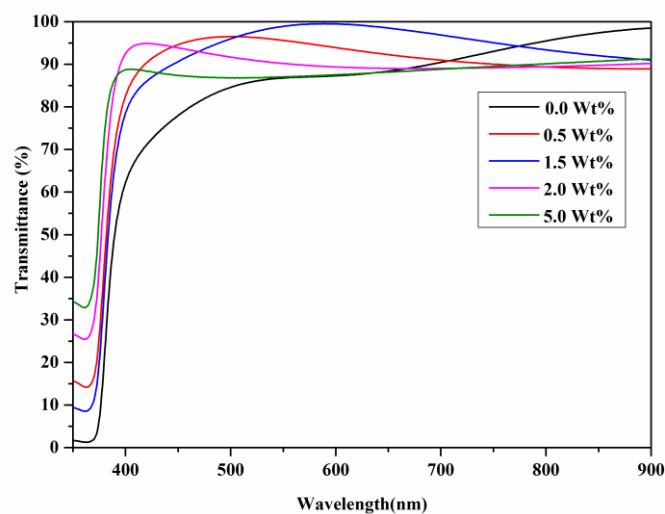


Fig.1. Transmittance spectra of ZnO thin films with different concentration (0-5wt%)

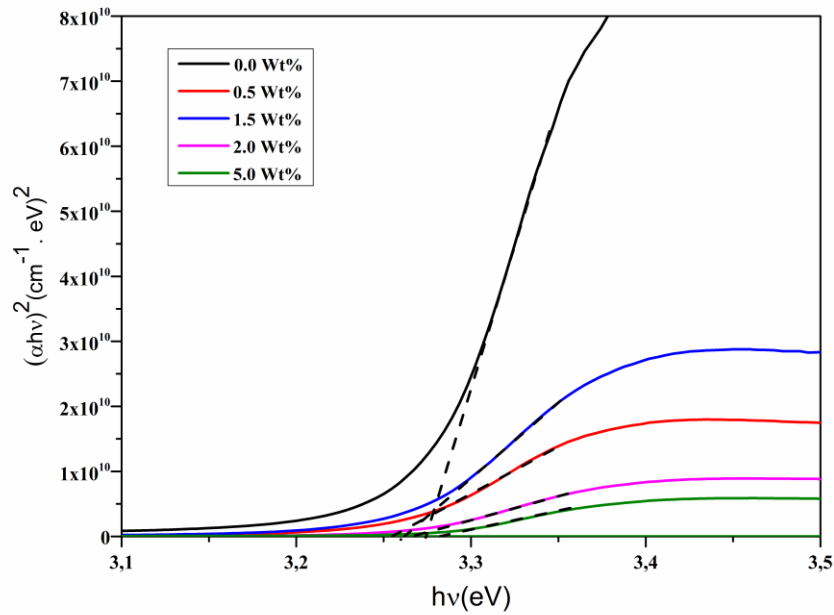


Fig.2. Plot of $(\alpha h\nu)^2$ versus $(h\nu)$ for the band gap determination for different concentration (0-5wt%).

We have used the band tail energy E_u , which characterizes the disorder defects in thin films, the band tail energy was calculated using the well know following relation:

$$\alpha = \alpha_0 \exp(h\nu / E_u)$$

where α is the absorption coefficient, α_0 is constant; $h\nu$ and E_u are photon energy and Urbach energy respectively. The Urbach energy was determined from the inverse of slop of $\ln(\alpha)$ versus $(h\nu)$, as depicted in Fig. 3. The found Urbach energy values varied between (88-104 meV), which are feeble values indicating the feeble disorder defects in thin films product. Compared between each other the Cu doped ZnO samples reveal high transmittance in the case of 2wt. % Cu doping which may be due to the less disorder in the product as illustrated in table 2.

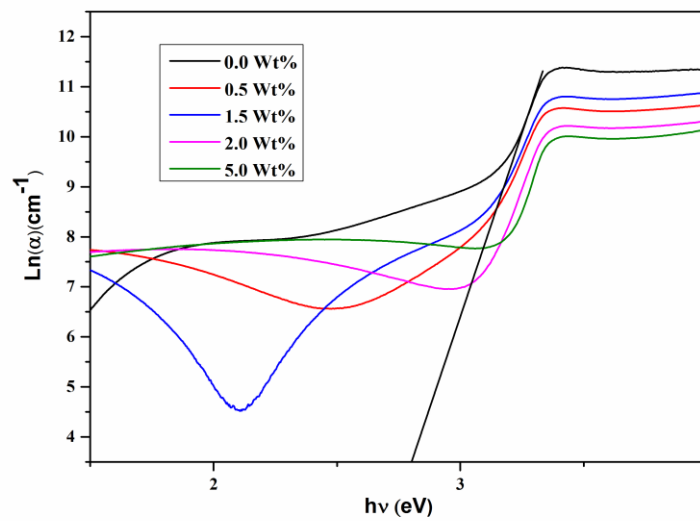


Fig.3. Plot of $(Ln\alpha)$ versus (hv) for the Urbach energy determination for different concentration (0-5wt%).

Table 2. Optical parameters for ZnO:Cu thin films.

Cu/Zn (wt%)	T%	$E_g(eV)$	$E_u(meV)$	$\delta (10^{+15}line/m^2)$
0.0	81.25	3.275	88.58	1.76
0.5	86.12	3.259	104.70	1.37
1.5	85.04	3.262	104.15	1.47
2.0	91.71	3.268	89.68	1.11
5.0	89.86	3.284	95.69	1.42

3.2 Structural analysis

Fig.4 shows the XRD patterns of (0-5wt%) Cu doped ZnO. The obtained diffraction peaks obviously exhibits the crystalline nature of ZnO with peaks corresponding to (100), (002), (101), (110) and (103) which are in good according with the standard Joint Committee Powder Diffraction JCPDS (Card No. 36-1451, space group $p6_3mc$) corresponding to hexagonal wurtzite structure of ZnO . As growth direction, c -axis (002) plane in all the thin films except ones (for 0.0 and 1.5 wt%) is the preferred. Comparing with undoped sample, one can detect from the XRD spectra that a small shift of the peaks towards the greater values of 2θ angles with (2 and 5 wt.%) Cu doped ZnO conforming the substitution of Zn^{2+} by Cu^{2+} in the lattice as seen in insert of Fig. 4. There are no additional or any peaks corresponding to copper. The averages size crystallite at (002) peaks were evaluated using Debye Sherrer's formula:

$$G = \frac{0.9\lambda}{\beta \cos \theta}$$

where λ , β and θ are the wavelength of X-ray, the full width at half maximum (*FWHM*) and the Bragg's angle of (*hkl*) reflections, respectively. The crystallite size of all thin films ZnO was averaged between (23-29 nm). After doping this average gradually increases with doping compared to the undoped ZnO. The maximum crystallite size was obtained with 2% wt Cu/Zn doping then decreases. For further information, the lattice parameter *c* is estimated using the following relations:

$$2d_{hkl} \sin \theta = n\lambda$$

and

$$\frac{1}{d^2_{hkl}} = \frac{4}{3} \left(\frac{h^2 + hk + k^2}{a^2} \right) + \frac{l^2}{c^2}$$

where *n* is the order of diffraction, *d_{hkl}* is the plane spacing and *hkl* are the Miller indices of the planes. Compared to undoped sample, there is slight decreasing in the lattice parameter *c* of ZnO matrix for (2 and 5 wt% doping) which can be attributed to replacement of Zn⁺² by Cu⁺² having ionic radius (0.73Å) into ZnO crystal lattice. The later is a less than Zn⁺² ionic radius (0.74 Å) leading to a decrease in the *d* inter spacing and unit cell. All those structural parameters of ZnO thin films are tabulated in Table 2

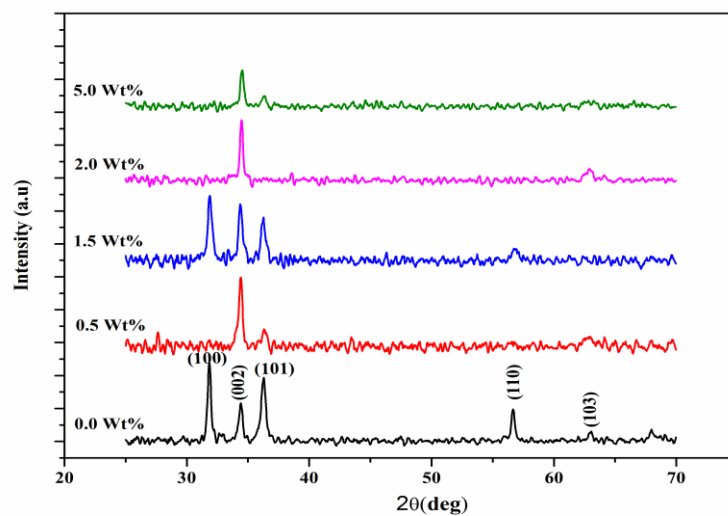


Fig. 4. X-ray diffraction pattern of ZnO thin films with different Cu concentration (0-5wt%), insert represents the shift of θ .

Table 2. Structural parameters for (0-5wt%) Cu doped ZnO thin films (c_0 is taken from JCPDS (Card No. 36-1451, space group $p6_3mc$))

Samples wt% Cu doping	2 θ	Lattice parameters(\AA)		Calculated d(\AA)	Average grain size (nm)
		c	$\Delta c=c-c_0$		
0.0	34.424	5.2089	0.0029	2.6045	23.82
0.5	34.417	5.2099	0.0039	2.6049	26.98
1.5	34.406	5.2117	0.0057	2.6058	26.02
2.0	34.488	5.1996	-0.0064	2.5998	29.99
5.0	34.538	5.1923	-0.0137	2.5961	26.54

4. Conclusion

In summary, undoped (ZnO) and copper doped ZnO thin films were deposited by spray pyrolysis technique with moving nozzle (homemade) onto glass substrate heated at 375°C. The optical study reveals that the average transmittance of all samples was more than 81% in the visible region, and becomes more transparent with Cu doping. Also optical gap energy predicted to be in 3.25-3.28eV range. XRD study indicated that all thin films are crystallized in a hexagonal wurtzite structure with a strong (002) preferred orientation except (for 0.0 and 1.5 wt%). A maximum value of crystallite size $G=29$ nm is attained with 2wt.% doping. As a result, Cu is a good doping quality for transparent ZnO thin films amelioration which may be widely applied in optoelectronic devices, etc.

References:

- [1] A. Djurišić, A.M.C. Ng, X. Chen, ZnO nanostructures for optoelectronics: material properties and device applications, *Progress in quantum electronics*, 34 (2010) 191-259.
- [2] V. Galstyan, E. Comini, C. Baratto, G. Faglia, G. Sberveglieri, Nanostructured ZnO chemical gas sensors, *Ceramics International*, 41 (2015) 14239-14244.
- [3] S.-Y. Lee, T. Hwang, S. Lee, W. Lee, B. Lee, J. Kim, S. Kim, H. Lee, H.-M. Lee, B. Park, Nanoroughness control of Al-Doped ZnO for high efficiency Si thin-film solar cells, *Current Applied Physics*, 15 (2015) 1353-1357.
- [4] J.-H. Lee, K.-H. Ko, B.-O. Park, Electrical and optical properties of ZnO transparent conducting films by the sol-gel method, *Journal of crystal growth*, 247 (2003) 119-125.
- [5] S. Kim, H. Moon, D. Gupta, S. Yoo, Y.-K. Choi, Resistive switching characteristics of sol-gel zinc oxide films for flexible memory applications, *Electron Devices, IEEE Transactions on*, 56 (2009) 696-699.
- [6] R. Yousefi, B. Kamaluddin, P. Room-temperature, spectra indicate that they have a potential application as properties of ZnO nanobelts, *Appl. Surf. Sci.*, 255 (2009) 9376-9380.
- [7] N. Yamamoto, H. Makino, S. Osone, A. Ujihara, T. Ito, H. Hokari, T. Maruyama, T. Yamamoto, Development of Ga-doped ZnO transparent electrodes for liquid crystal display panels, *Thin Solid Films*, 520 (2012) 4131-4138.
- [8] G.M. Ali, P. Chakrabarti, ZnO-based interdigitated MSM and MISIM ultraviolet photodetectors, *Journal of Physics D: Applied Physics*, 43 (2010) 415103.
- [9] K. Raja, P. Ramesh, D. Geetha, Synthesis, structural and optical properties of ZnO and Ni-doped ZnO hexagonal nanorods by Co-precipitation method, *Spectrochimica Acta Part A: Molecular and Biomolecular Spectroscopy*, 120 (2014) 19-24.

- [10] S. Fabbiyola, L.J. Kennedy, U. Aruldoss, M. Bououdina, A. Dakhel, J. JudithVijaya, Synthesis of Co-doped ZnO nanoparticles via co-precipitation: Structural, optical and magnetic properties, *Powder Technology*, 286 (2015) 757-765.
- [11] G.E. Fernandes, D.-J. Lee, J.H. Kim, K.-B. Kim, J. Xu, Infrared and microwave shielding of transparent Al-doped ZnO superlattice grown via atomic layer deposition, *Journal of Materials Science*, 48 (2013) 2536-2542.
- [12] M. Arshad, M.M. Ansari, A.S. Ahmed, P. Tripathi, S. Ashraf, A. Naqvi, A. Azam, Band gap engineering and enhanced photoluminescence of Mg doped ZnO nanoparticles synthesized by wet chemical route, *Journal of Luminescence*, 161 (2015) 275-280.
- [13] C. Boukaous, B. Benhaoua, A. Telia, S. Ghanem, Effect of copper doping sol-gel ZnO thin films: physical properties and sensitivity to ethanol vapor, *Materials Research Express*, 4 (2017) 105024.
- [14] A. Abdulrahman, STUDY THE OPTICAL PROPERTIES OF THE VARIOUS DEPOSITION SOLUTIONS OF ZnO NANORODS GROWN ON GLASS SUBSTRATE USING CHEMICAL BATH DEPOSITION TECHNIQUE, *Journal of Ovonic Research Vol*, 16 (2020) 181-188.
- [15] Z. Fang, Y. Tan, H. Gong, C. Zhen, Z. He, Y. Wang, Transparent conductive Tb-doped ZnO films prepared by rf reactive magnetron sputtering, *Materials Letters*, 59 (2005) 2611-2614.
- [16] M. Salah, S. Azizi, A. Boukhachem, C. Khaldi, M. Amlouk, J. Lamloumi, Effects of lithium doping on: microstructure, morphology, nanomechanical properties and corrosion behaviour of ZnO thin films grown by spray pyrolysis technique, *Journal of Materials Science: Materials in Electronics*, 30 (2019) 1767-1785.
- [17] M. Tliba, A. Benhaoua, R. Gheriani, B. Benhaoua, A. Rahal, C. Boukaous, A. Tliba, La-DOPED ZNO THIN FILMS PREPARED BY SPRAY PYROLYSIS WITHMOVING NOZZLE: STUDY OF PHYSICAL PROPERTIES AND ADSORPTION ABILITY OF THE COPPER, *DIGEST JOURNAL OF NANOMATERIALS AND BIOSTRUCTURES*, 13 (2018) 991-1002.
- [18] B. Benhaoua, A. Rahal, S. Benramache, The structural, optical and electrical properties of nanocrystalline ZnO: Al thin films, *Superlattices and Microstructures*, 68 (2014) 38-47.
- [19] C. Bates, W. White, R. Roy, The solubility of transition metal oxides in zinc oxide and the reflectance spectra of Mn²⁺ and Fe²⁺ in tetrahedral fields, *Journal of Inorganic and Nuclear Chemistry*, 28 (1966) 397-405.
- [20] R. Baghdad, B. Kharroubi, A. Abdiche, M. Bousmaha, M. Bezzerrouk, A. Zeinert, M. El Marssi, K. Zellama, Mn doped ZnO nanostructured thin films prepared by ultrasonic spray pyrolysis method, *Superlattices and Microstructures*, 52 (2012) 711-721.
- [21] R. Elilarassi, G. Chandrasekaran, Synthesis and optical properties of Ni-doped zinc oxide nanoparticles for optoelectronic applications, *Optoelectronics letters*, 6 (2010) 6-10.
- [22] K.J. Kim, Y.R. Park, Spectroscopic ellipsometry study of optical transitions in Zn 1- x Co x O alloys, *Applied Physics Letters*, 81 (2002) 1420-1422.
- [23] J. Diouri, J. Lascaray, M. El Amrani, Effect of the magnetic order on the optical-absorption edge in Cd 1- x Mn x Te, *Physical Review B*, 31 (1985) 7995.
- [24] M. Ferhat, A. Zaoui, R. Ahuja, Magnetism and band gap narrowing in Cu-doped ZnO, *Applied Physics Letters*, 94 (2009) 142502.
- [25] E. Burstein, Anomalous optical absorption limit in InSb, *Physical Review*, 93 (1954) 632.
- [26] H.F. McMurdie, M.C. Morris, E.H. Evans, B. Paretzkin, W. Wong-Ng, L. Ettliger, C.R. Hubbard, Standard X-ray diffraction powder patterns from the JCPDS research associateship, *Powder Diffraction*, 1 (1986) 64-77.